

Article

Synthesis and Characterization of Epoxidized Beechwood Pyrolysis Bio-Oil as a Curing Agent of Bio-Based Novolac Resin

Jie Xu , Nicolas Brodu, Lokmane Abdelouahed , Chetna Mohabeer  and Bechara Taouk * 

INSA Rouen Normandie, Univ Rouen Normandie, Normandie Université, LSPC, UR 4704, F-76000 Rouen, France

* Correspondence: bechara.taouk@insa-rouen.fr; Tel.: +33-232-956-650

Abstract: A bio-oil-based epoxy (BOE) resin was synthesized using phenolic compounds from beechwood pyrolysis oil. These compounds were separated from crude pyrolysis oil by coupling two methods: fractional condensation and water extraction. The chemical structure of the BOE resin was characterized by NMR and FTIR analyses. BOE resin was used as a curing agent of bio-oil glyoxal novolac (BOG) resin to gradually replace bisphenol A diglycidyl ether (DGEBA). The thermal properties of cured resins and kinetic parameters of the curing reaction using differential scanning calorimetry (DSC) were discussed. Incorporating the BOE resin resulted in a lower curing temperature and activation energy compared to using DGEBA. These results indicate that the water-insoluble fraction of pyrolysis oil condensate can potentially be used to synthesize high-thermal performance and sustainable epoxidized pyrolysis bio-oil resins and also demonstrate its application as a curing agent of bio-oil glyoxal novolac (BOG) resin.

Keywords: beechwood biomass; upgraded pyrolysis bio-oil; bio-oil-based glyoxal novolac resin; bio-oil-based epoxy resin; curing kinetics



Citation: Xu, J.; Brodu, N.; Abdelouahed, L.; Mohabeer, C.; Taouk, B. Synthesis and Characterization of Epoxidized Beechwood Pyrolysis Bio-Oil as a Curing Agent of Bio-Based Novolac Resin. *Fuels* **2023**, *4*, 186–204. <https://doi.org/10.3390/fuels4020012>

Academic Editor: Maria A. Goula

Received: 11 January 2023

Revised: 13 March 2023

Accepted: 10 April 2023

Published: 15 May 2023



Copyright: © 2023 by the authors. Licensee MDPI, Basel, Switzerland. This article is an open access article distributed under the terms and conditions of the Creative Commons Attribution (CC BY) license (<https://creativecommons.org/licenses/by/4.0/>).

1. Introduction

Epoxy resin is one of the most significant thermosetting polymers having excellent mechanical, thermal, and electrical properties, high adhesion strength, corrosive resistance, favorable processing ability, and low curing shrinkage. It is widely used in adhesives, coatings, encapsulation, composite materials, and packaging materials for electronic devices [1–5].

Depending on the different epoxy equivalent weights, molecular weights, and viscosities, various types of epoxy resins can be found on the market. Bisphenol A glycidyl ether (DGEBA) is the most widely used epoxy resin, accounting for more than 90% of the global epoxy resin market [6]. However, DGEBA is a toxic and petroleum-derived organic compound, as it is derived from bisphenol A (BPA). The replacement of BPA with alternatives from sustainable and renewable resources, such as bio-based polyphenols, is highly desired [7–11].

Researchers have recently been focusing on developing bio-based epoxy monomers or oligomers to replace the traditional DGEBA by investigating high-performance materials [12,13]. These bio-based epoxy resins have been prepared from a variety of renewable resources, such as vegetable oils (soybean oil, linseed oil, palm oil, and castor oil) [14–16]. Several promising results on the application of woody biomass to the production of epoxy resins have also been reported [17]. Zhang et al. [18] prepared an epoxy grouting resin using lignin, which is an underutilized by-product of the forestry industry that has outstanding viscosity with a low mechanical property. Another potential eco-friendly substitute for BPA is bio-oil from biomass pyrolysis [19]. Bio-oil produced by hydrothermal liquefaction of loblolly pine has been used for the synthesis of a bio-oil-based epoxy resin [7].

Bio-oil is a complex liquid mixture with over 255 different chemical compounds that can be classified into different “families” after identification; these include phenols, carboxylic acids, ketones, esters, alcohols, sugars, aldehydes, and furans, among others [20].

However, the application of phenol obtained from pyrolysis oil is limited due to fewer reactive sites and steric hindrance. For this reason, it is very necessary to upgrade bio-oil [19,21–25]. In our previous study [26], the combination of the two environmentally friendly methods (fractional condensation and water extraction) was successful in separating phenolic compounds from beechwood pyrolytic oil. The extraction of bio-oil by water was able to separate phenol into water-insoluble fractions based on the broad range of dew points and the different polarities and affinities with water [27,28]. As bio-oil comprises a large yield of phenolics, it will surely become a very effective alternative to commercial BPA in the field of epoxy resin production [29].

Now, the polymerization of phenol and formaldehyde under acidic conditions leads to the production of a novolac-type resin, which needs to be cross-linked by a curing agent [30]. Considering the decomposition of hexamethylenetetramine (ammonia and formaldehyde), which is the most common curing agent during heating, there is an urgent need to develop an environmentally friendly curing agent [31].

In our previous research, the water-insoluble fraction of bio-oil fractional condensation products was successfully used for the synthesis of novolac-type resins (BOG) with glyoxal, and they were successfully cured with DGEBA [32]. In this study, the potential of a synthesized epoxidized bio-oil resin as a curing agent of the bio-based glyoxal novolac resin is evaluated and discussed. Firstly, the water-insoluble fraction of the bio-oil fractional condensation products were polymerized with epichlorohydrin to prepare BOE resin. The chemical structure of BOE resin was confirmed by FT-IR, GPC, and ¹H-NMR spectroscopy. In addition, the BOE resin gradually replaced DGEBA as a bio-based formaldehyde-free cross-linker for bio-based glyoxal novolac resin to build a “greener” bio-based material. In order to determine the kinetic parameters of the curing reaction, model-free methods were applied to the data obtained from differential scanning calorimetry (DSC). A comparison between the thermal properties of BOE/DGEBA cured BOG resins was carried out. To the best of our knowledge, a synthesized bio-based epoxy resin based on the upgraded beechwood pyrolysis oil has been used for the first time in this study. The aim was to gradually replace the DGEBA equivalent as a formaldehyde-free cross-linker for bio-based novolac resin to produce a 100% bio-oil-based green material.

2. Experimental Section

2.1. Materials

Epichlorohydrin (ECH, 99%), benzyltriethylammonium chloride (TEBAC), glyoxal (40%), oxalic acid ($\geq 99\%$), ethanol ($\geq 99\%$), acetone ($\geq 99\%$), sodium hydroxide (NaOH), potassium hydroxide (KOH), pyridine, dichloromethane (DCM), acetic anhydride ($>95\%$), diglycidyl ether of bisphenol A (DGEBA) ($\geq 99\%$), and triphenylphosphine (TPP) ($\geq 95.0\%$) used for experiments were all purchased from Sigma Aldrich (St. Louis, MO, USA).

2.2. Beech Wood Pyrolysis Bio-Oil Fractions

Figure 1 shows the recapitulation of the biomass pyrolysis operation and separation method, which has already been reported in our previous work [26]. Intermediate beechwood pyrolysis was performed in a drop tube reactor (DTR), and the products were collected (bio-oil, biochar, and biogas). A 3-condenser system (temperatures set at 110, 20, and -11 °C) was connected to trap the oil fractions (OIL1, OIL2, and OIL3, respectively). Then, OIL1 was selected in order to recover the water-insoluble fraction (OIL1WI), which was in turn collected simply by adding 70 wt.% of water, then centrifugating, and separating. Vacuum drying at 105 °C was then performed to remove water. The potential of OIL1WI as a promising stable bio-oil fraction for resin synthesis was already known based on previous results [32,33].

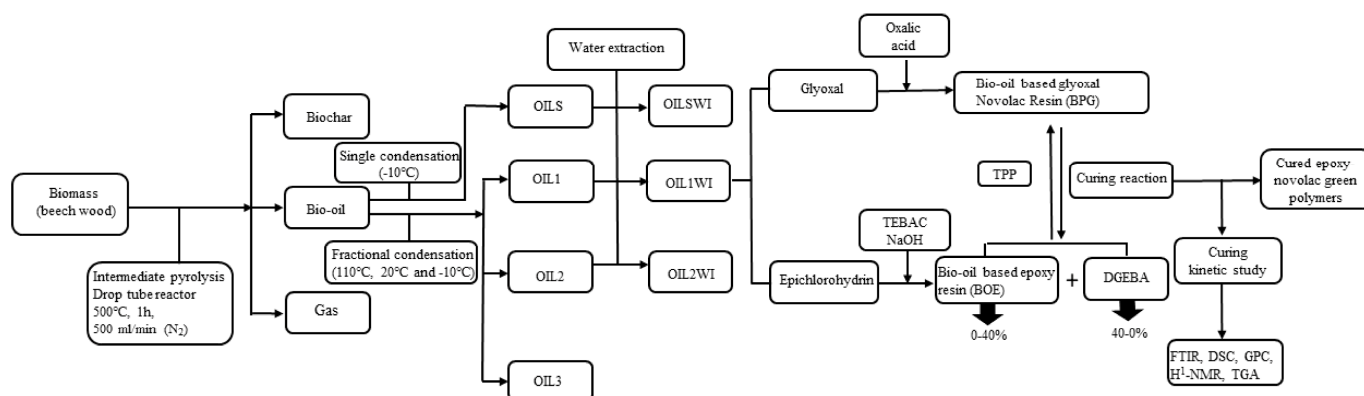


Figure 1. Overview of bio-oil production process and resin synthesis-curing system.

The recovered bio-oil fractions were analyzed by using a GC-MS (Varian 3900-Saturn 2100T), while a GC-FID (Scion 456-GC Bruker instrument, Billerica, MA, USA) was applied to quantify the identified components; the calculation method to determine molar fraction of phenolic compounds was detailed in our previous work [26]. During these analyses, the main phenols were identified and quantified, and the hydroxyl number was calculated (Table 1).

Table 1. Molar fraction (mol.%) of GC-FID detected phenolic compounds in oil and hydroxyl number (average of triplicate runs with a standard deviation < 3%).

| Phenols in Oil | mol.% | |
|-------------------------------------|-------|--------|
| | OIL1 | OIL1WI |
| Phenol | 1.20 | 2.47 |
| o-Cresol | 1.20 | 3.26 |
| m-Cresol | 0.94 | 1.91 |
| 2,6-Dimethylphenol | 1.10 | 1.86 |
| 2,4-Dimethylphenol | 3.59 | 5.06 |
| Phenol, 3-ethyl-5-methyl- | 1.00 | 2.42 |
| 3-Methylcatechol | 2.62 | 2.57 |
| Catechol | 2.88 | 3.14 |
| 4-Methylcatechol | 1.88 | 3.08 |
| 4-Ethylcatechol | 1.69 | 5.52 |
| Guaiacol | - | - |
| Creosol | 1.69 | 3.58 |
| 4-Ethylguaiacol | 1.59 | 3.02 |
| Syringol | 3.06 | 4.71 |
| Isoeugenol | 1.55 | 3.21 |
| 2,4-Dimethoxyphenol | 1.30 | 4.62 |
| Hydroxyl group/mmol·g ⁻¹ | 3.62 | 7.62 |

2.3. Synthesis of Bio-Oil Based Glyoxal Novolac Resin

The polymerization of bio-oil (OIL1WI) glyoxal (BOG) resin was conducted using glyoxal as an aldehyde precursor to replace formaldehyde and the OIL1WI fraction as the phenol precursor, as shown in Figure 1. The total concentration of phenolic compounds present in OIL1WI was calculated to be 5.80 mmol·g⁻¹.

All experiments were carried out in a 100 mL 3-neck reactor equipped with a condenser, a nitrogen inlet, and pressure-equalizing dropping funnel placed at the middle neck and 2 side necks. An oil bath was used to preheat the phenol precursors melted (70 °C), and then, the temperature was increased to 125 °C under atmospheric pressure, and agitation was ensured through a magnetic stirrer at a speed of 300 rpm. Oxalic acid (10 mol.%) was added to obtain acidic conditions. The molar ratio of phenol to glyoxal precursors was set as

2, and the glyoxal was added drop-wise through the pressure-equalizing dropping funnel; the same ratio was fixed for each experiment. The reaction medium was continuously agitated for 7 h. The resin was produced by rinsing 3 times with distilled water, then the unreacted monomer and acid were removed by drying under vacuum at 125 °C for 24 h. In addition, the yield of resin products was calculated according to the following equation:

$$\text{Yield}(\%) = \frac{\text{weight of final resin}}{\text{weight of reactant added}} \times 100\% \quad (1)$$

2.4. Synthesis of Bio-Oil-Based Epoxy Resin

The BOE resins were synthesized by a two-step glycidylation method [34,35]. A schematic of the resin synthesis is shown in Figure 2. Approximately 2 g (1.52×10^{-2} mol) of OIL1WI, used as an alternative to phenol, was added into a 100 mL glass reactor, followed by Epichlorohydrin (4 M eq/hydroxyl). The temperature gradually increased to 100 °C under continuous stirring. Then, a phase transfer catalyst, benzyltriethylammonium chloride (TEBAC, 0.012 M eq/hydroxyl), was introduced, and the reaction was left for 1 h. During the second step, the temperature decreased to 30 °C. The same TEBAC as before and a 20 wt.% aqueous solution of sodium hydroxide (2 M eq/hydroxyl) were mixed and added drop-wise through the pressure-equalizing dropping funnel. The reaction continued for 1–2 h at 30 °C. The organic layer was successively washed three times with water and poured into an extraction funnel to separate the water and remove the salt. A rotary evaporator was used at 90 °C to remove unreacted ECH. The resin products were finally dried and concentrated at 50 °C overnight. Each experiment was repeated three times, and the average values are reported. The yield of the bio-oil-based epoxy resins was determined by using the following equation [10]:

$$\text{Yield}(\%) = \frac{S}{L(1 + 0.427)} \times 100 \quad (2)$$

where S is the weight of the dried BOE, L is the weight of the dried OIL1WI, and 0.427 g is the stoichiometric amount of epichlorohydrin for 1 g of OIL1WI.

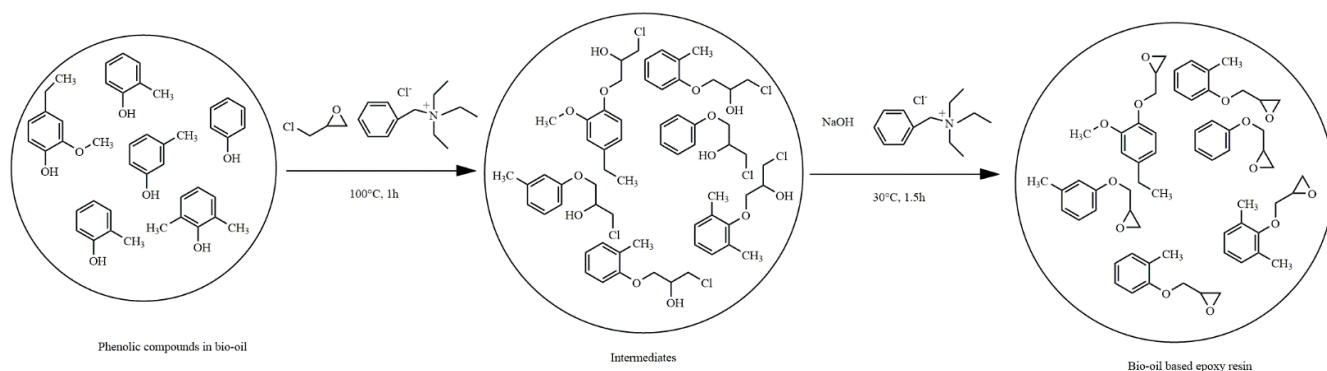


Figure 2. Schematic of the epoxy resin synthesis.

A specific amount of NaOH is beneficial to the reaction, while an excess amount will increase the probability of self-polymerization of ECH [36]. The molar ratio of NaOH/OHN and TEBAC/OHN and the reaction temperature were based on previous studies [34,35].

2.5. Curing Process

Non-isothermal DSC measurement has been widely applied to study the curing behavior and kinetics of resins and polymers [37–39]. Dynamic experiments were carried out at different heating rates (5, 10, 15, and 20 °C/min) from 25 to 250 °C to study the epoxy-novolac resin system, and the curing reaction of the BOG resins with 40 wt.% BOE/DGEBA

(based on the weight of the BOG resin) was determined by DSC. The obtained data were used in the additional kinetic study.

Firstly, the vacuum-dried BOG resin samples were dissolved in acetone and uniformly mixed with 40% of DGEBA as curing agent at the beginning and then gradually replaced by BOE. A total of 2% TPP was used as catalyst. The quantification of all the chemicals was based on the quantity of the BOG resin. Then, the mixture was left at room temperature for 12 h, allowing the evaporation of solvent. A sample of about 5 mg in a sealed aluminum crucible was heated in a N₂ environment to obtain the heating cycles. The onset and peak temperatures of curing and the reaction enthalpy were determined from the exothermic peak of curing and its linear integration, respectively, using the TA Universal analysis software. The amount of curing agent was optimized by testing, according to our previous studies [32]; finally, 40 wt.% of DGEBA was selected to obtain a higher T_g (117.39 °C) and a lower curing reaction temperature. The same quantity of DGEBA was then replaced by BOE resin.

The results obtained from the DSC measurements were then employed to calculate kinetics parameters according to the following equations (Equations (3)–(5)) by the model-free methods: Kissinger, Flynn–Wall–Ozawa (FWO), and Crane [21,40,41].

$$\text{Kissinger equation} \quad \ln\left(\frac{\beta}{T_p^2}\right) = \ln\left(\frac{AR}{E}\right) - \frac{E_a}{RT_p} \quad (3)$$

$$\text{Ozawa equation} \quad \log \beta = -\frac{0.4567E_a}{RT_p} + C \quad (4)$$

$$\text{Crane equation} \quad \frac{d \ln \beta}{d(1/T_p)} = -\frac{E_a}{nR} \quad (5)$$

T_p corresponds to the maximum reaction rate or peak temperature (K), β is the heating rate (K/min), E_a is the activation energy (kJ/mol), and R is the gas constant (8.314 J/mol·K). A, C, and n are the pre-exponential factor (min⁻¹), a constant, and the order of the curing reaction, respectively.

A resin-curing reaction was also conducted by putting the resin and curing agent mixture in the oven to evaluate additional properties of the cured resins. The temperature set program was 120 °C for 30 min, 150 °C for 30 min, and 180 °C for 1 h [39].

2.6. Characterization

2.6.1. Attenuated Total Reflection Fourier-Transform Infrared (ATR-FTIR)

ATR-FTIR spectroscopy was applied to verify the formation and change of the functional group in the bio-oil and resin samples (before and after curing). The spectrum was recorded in reflectance mode between 450–4000 cm⁻¹ at a resolution of 4 cm⁻¹ using a SHIMADZU IRTracer–100 spectrometer.

2.6.2. Nuclear Magnetic Resonance (¹H-NMR)

The resins were also characterized by ¹H-NMR spectroscopy. The spectra were recorded on a Bruker AVANCE III system (300 MHz). Additionally, 50 mg samples were dissolved in 0.4 mL d₆-DMSO with slight heating, and the samples were stirred until they were completely dissolved.

2.6.3. Epoxy Equivalent Weight (EEW) Determination

EEW is the weight of the resin (in g) that contains 1 g equivalent of the epoxide group. The epoxy equivalent of the BOE resin was determined by the reaction of an aliquot of standard pyridine hydrochloride in excess pyridine at reflux and subsequent back titration with standard sodium hydroxide-ethanol. Approximately 0.25 g of the BOE resin sample was taken and put in a 100 mL flask. Then, 25 mL of a solution of 0.2 mol/L hydrochlorides in pyridine was prepared and added to the flask. The contents of the flask were stirred

and heated under reflux at 115 °C for 20 min to dissolve the epoxy sample. After cooling down, the titration of the excess acid was carried out by a prepared 0.2 mol/L sodium hydroxide-ethanol solution using a pH meter to follow the pH value of the solution until it reached 13. The pH value was recorded each time 1 mL was added, and a graph was plotted to determine the volume of solvent added when the maximum change in the pH value occurred. A blank assay was performed under the same conditions in the absence of the BOE resin. The EEW was calculated by using Equation (6).

$$EEW = \frac{P \times 10^3}{(V_A - V_B) \times C_{NaOH}} \quad (6)$$

where P = BOE resin weight (g); V_A = 0.2 mol/L NaOH volume (mL) for the blank; V_B = 0.2 mol/L NaOH volume (mL) for the prepolymer; C_{NaOH} = Molar concentration of 0.2 mol/L NaOH solution.

2.6.4. Gel Permeation Chromatography (GPC)

The average molecular weight (M_w) and average molecular weight number (M_n) of the resin samples were measured by Waters Breeze gel permeation chromatography (Waters, Milford, MA, USA, 1525 binary HPLC pump, RI detector at 270 nm, Waters Styragel HR1 column at 40 °C). DCM was employed as the eluent at a flow rate of 1 mL/min, and polystyrene was chosen as the calibration standard [19,40–42]. Resin samples were prepared by dissolving 3 mg/mL in DCM and then filtering with a 0.45 µm nylon membrane. Later, the samples were injected into the GPC instrument, and the results were collected.

2.6.5. Thermal Analysis of the Cured Resins

The thermal properties were characterized by DSC (TA Q1000 instrument) by placing approximately 5 mg of the sample in a sealed hermetic crucible with purging with nitrogen gas at 50 mL/min. Samples were cycled between 25 and 200 °C at a heating/cooling rate of 5 °C/min. After that, the glass transition temperature (T_g) was measured.

The thermogravimetric analysis (TGA) was secondly used to monitor the thermal degradation of a sample of the cured resin. By using a TA Q600 TGA instrument, 5–10 mg of the sample was heated to 105 °C, equilibrated for 5 min and then heated up to 900 °C with a heating rate of 10 °C/min under a high purity nitrogen flow of 50 mL/min.

3. Results and Discussion

3.1. Synthesis and Characterization of the Bio-Oil Based Epoxy (BOE) Resin

BOE resin was synthesized by reacting bio-oil water-insoluble fractions with epichlorohydrin (ECH), as shown in Figure 2. After purification, the obtained BOE resin was a black semi-solid.

According to the literature [43], the epoxidation reaction can be divided into two steps (as shown in Figure 2). In the first step, a phase transfer catalyst (TEBAC) was used to form ion pairs, which further underwent an addition reaction with ECH to open the epoxy ring and then reacted with OH groups in the bio-oil [7]. In the second step of the reaction, the same quantity of TEBAC was added. NaOH was used as a catalyst, and its main function was to dihydrochloride the intermediates (ring-closing) and neutralize HCl.

The FTIR spectra (Figure 3) show the differences in the functional groups of the BOE resin, ECH, and their phenolic precursors (bio-oil). The signals at 911 and 855 cm^{-1} belong to the oxirane group [7,44], and they can be clearly found in ECH. However, there was no signal detected in the spectrum of the bio-oil. After resinification, there were some new peaks that appeared in the spectrum of the resulting BOE resin. These peaks confirmed the successful epoxidation reaction between phenols in the bio-oil and ECH to form the new epoxy ring in the resin structure. Furthermore, concerning the C–O–C group, deformation peaks were observed in the range of 1225–1250 cm^{-1} and asymmetric and symmetric bending can be found in the range of 1026–1043 cm^{-1} .

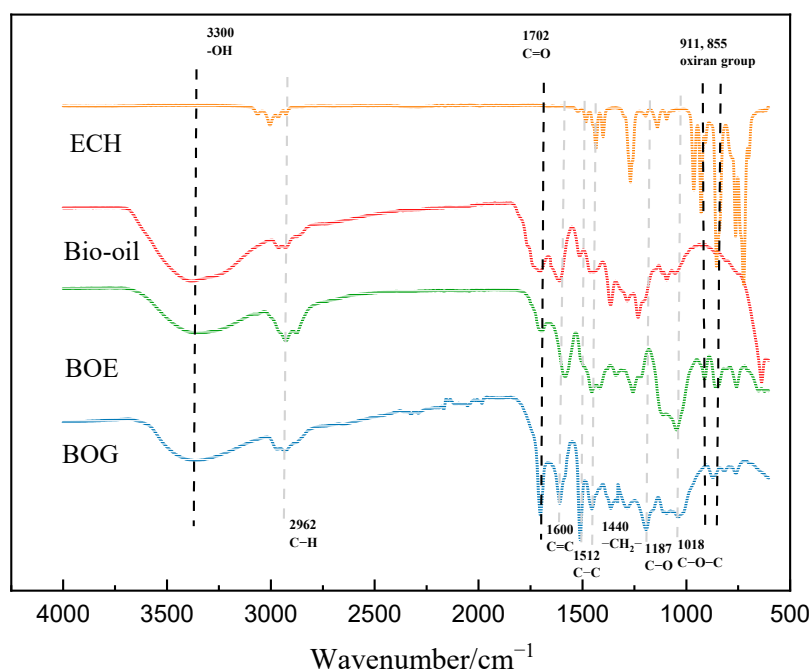


Figure 3. FTIR spectra of ECH, OIL1WI, BOG resin, and BOE resin.

There is a broad peak around 3300 cm^{-1} , belonging to the O–H stretching vibrations, which was diminished for the BOE resin compared to the bio-oil due to the conversion of the phenolic hydroxyl function into the glycidyl one. According to our previous analysis of bio-oil, the band correlating to the aldehyde group in the bio-oil appeared at 1702 cm^{-1} [26]. This also decreased after the reaction, indicating that a condensation reaction occurred.

The $^1\text{H-NMR}$ spectrum of the BOE resin also confirmed the successful epoxidation reaction of the bio-oil, as shown in Figure 4. The $^1\text{H-NMR}$ spectrum of OIL1WI and BOG resin has also been shown in Figure A1, in the Appendix A, as a reference. The signals at 2.50 ppm belong to the DMSO-D_6 solvent. The protons from the benzene ring skeleton and the phenol hydroxyl, which come from the phenolic compounds in bio-oil, were found in the BOE resin, and their signals are between 7.5 and 6 ppm (d, e, f) in the spectrum [45]. In addition, the signals at 3.37 ppm (h) indicate the presence of aromatic methoxy protons ($-\text{OCH}_3$) related to the presence of guaiacols in the bio-oil [46]. As expected, the strong signals between 1.5 and 0.5 ppm represent protons ascribed to the aliphatic chain linked to the small molecules in the bio-oil. The peaks at 1.57 and 2.08 ppm correspond to the alkyl protons in the backbone of the phenolics [47]. Furthermore, the signals around 3.30 and 2.82 ppm are attributed to the protons of oxirane moieties. The protons at a and b are on the epoxide CH_2 (O)–CH– structure, and the peaks of the protons (c) on the $-\text{CH}_2-$ next to the epoxy group at around 4 ppm were observed as well [48–51], which demonstrated that the target compounds were synthesized successfully.

The yield and EEW are two important parameters for epoxy resin. The yield reflects the degree of the polymerization reaction, while the EEW indicates the reactivity of the epoxy resin. A lower EEW is desirable because it means that a higher concentration of the epoxide group is attached to the resin. It should also be noted that the reaction time of the second step was reported to be an influencing factor on the yield and EEW [36,52]. To maximize the yield and minimize the EEW value of the polymerization under the selected reaction condition, various reaction times (1.5, 2, and 2.5 h) were chosen and examined (Table 2). It was evident that a longer reaction time resulted in a higher yield and EEW value of the epoxy resins. These results are in agreement with the literature [7,36]. To optimize the EEW value and yield at the same time, the optimal time for the ring close reaction was determined to be 2 h.

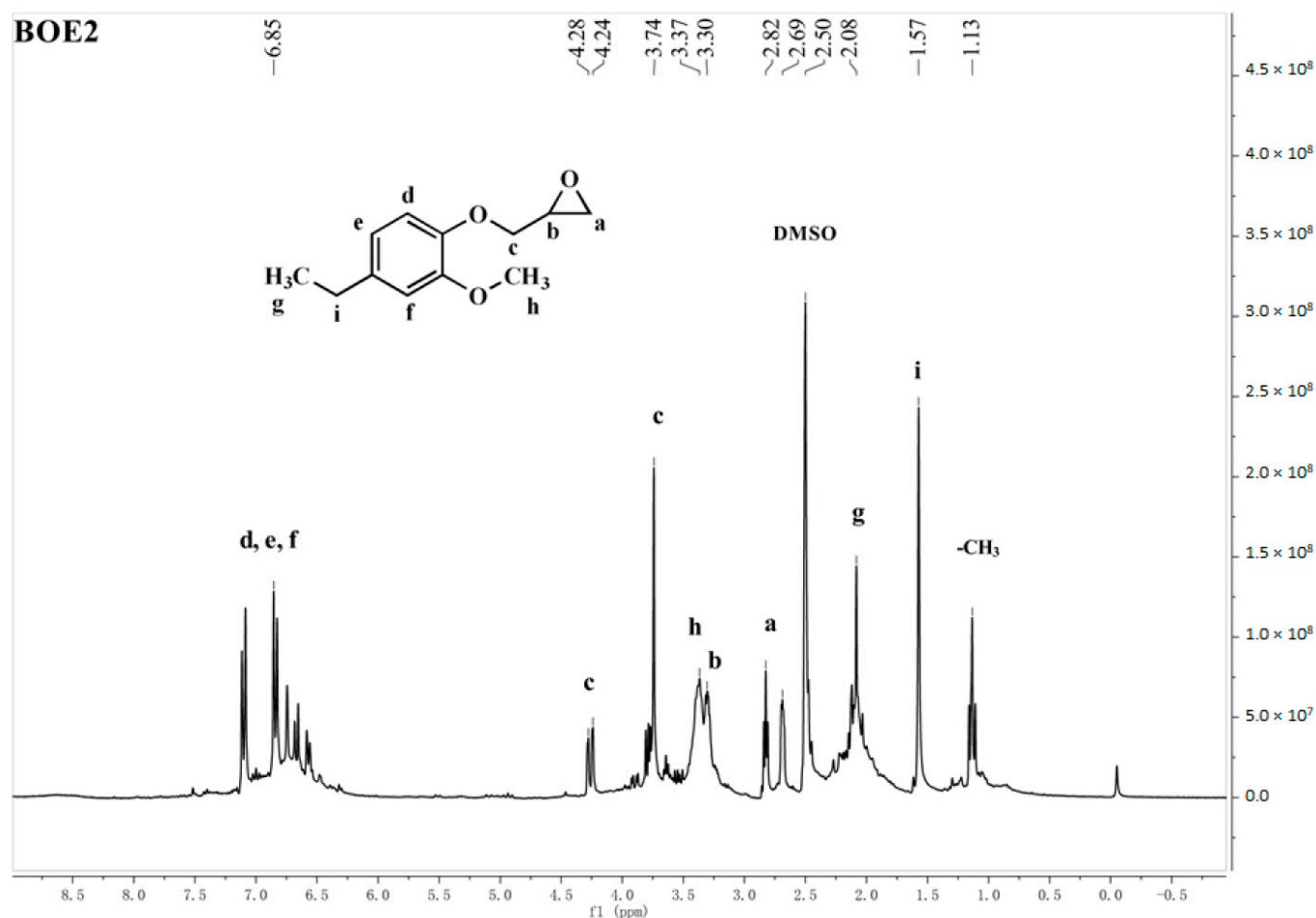


Figure 4. $^1\text{H-NMR}$ spectrum of the BOE resin.

Table 2. Yield and EEW of epoxy resins.

| Epoxy Resin | Reaction Time/h | Yield (%) | EEW (g Equiv $^{-1}$) | M_n (g/mol) | M_w (g/mol) | Polydispersity |
|-------------|-----------------|----------------|------------------------|---------------|---------------|----------------|
| BOE1.5 | 1.5 | 87.3 \pm 2.2 | 310 \pm 3 | 303 \pm 20 | 723 \pm 15 | 2.39 |
| BOE2 | 2.0 | 91.0 \pm 1.7 | 317 \pm 2 | 368 \pm 18 | 1019 \pm 31 | 2.77 |
| BOE2.5 | 2.5 | 92.8 \pm 1.1 | 375 \pm 1 | 375 \pm 11 | 1108 \pm 33 | 2.96 |
| DGEBA | - | - | 181 \pm 1 | - | - | - |

As the OIL1WI fraction was a mixture of monomeric, oligomeric, and macromolecular phenolic components, it had a higher molecular weight and a lower phenolic hydroxyl reactivity than commercial phenols. In addition, the EEW of DGEBA was also determined by the titration method, and BOE showed a higher EEW than DGEBA, which is a commercially manufactured epoxy resin with a desired EEW (181).

The molecular weight distribution (as shown in Table 2) of the BOE resins was obtained by the GPC chromatograms; the GPC profile of the BOE2 resin is shown separately in Figure A2. The difference between the M_w and M_n values of the BOE2 resin ($M_w = 1019 \pm 31$ g/mol, $M_n = 368 \pm 18$ g/mol) resulted in a large polydispersity (2.77). Various substituents of phenolics in the bio-oil limited their activity, and it was difficult for some of them (e.g., 4-ethylguaiacol) to participate in the further cross-linking reaction due to the addition of the methoxy group that increased their steric hindrance. Moreover, the strong presence of small molecules in the bio-oil reduced the value of M_n . Meanwhile, the glycidylation reaction occurred, leading to the formation of oligomers. These newly formed glycidyl groups can react with the phenolic group of another molecule to create

higher molecular weight oligomers [9,18]. This can result in an epoxy resin with a large polydispersity. Moreover, the change in the molecular weight was related to the EEW value and the yield of the epoxy resins (as can be seen in Table 2).

3.2. Characterization of BOG Resin

Similar to the BOE resin, OIL1WI was also used as a phenol precursor to replace pure phenol to synthesize the BOG resin. After drying, the obtained BOG resin was a black-colored solid.

The FTIR spectra illustrate the functional groups in the BOG resin (Figure 3) and the assignment of the corresponding bands. Based on the structure of the resin (Figure 2), the methylene group ($-\text{CH}_2-$), aldehyde group ($\text{C}=\text{O}$), carbon-carbon double bond ($\text{C}=\text{C}$), aromatic $\text{C}-\text{C}$, and ether group ($\text{C}-\text{O}-\text{C}$) were identified according to the stretching modes at 2962, 1702, 1600, 1512, 1440, 1187, and 1018 cm^{-1} , respectively, which indicate the condensation reaction between the aldehyde in glyoxal and phenols to form $-\text{CH}_2-\text{C}=\text{O}$ and $-\text{C}=\text{C}-\text{O}-\text{C}=\text{O}$. These two different linkages were formed during polymerization [53]. Additionally, these peaks appeared in the spectrum of the BOG resin, indicating that the synthesis was successful. A comparison shows that there were some differences between the bio-oil and BOG resin, including the obvious increase in the peaks at 2962, 1702, 1187, and 1018 cm^{-1} . The absorptions at 1300–1000 cm^{-1} were due to $\text{C}-\text{O}-\text{C}$ stretching, which could be found in the bio-oil and BOG resin, related to the methoxy group of guaiacols. The signals at 871, 825, and 760 cm^{-1} belonged to out-of-plane bending of the aromatic $\text{C}-\text{H}$ bonds [24]. The $\text{O}-\text{H}$ stretching at around 3300 cm^{-1} and the $\text{C}-\text{O}$ stretching of aromatics at 1210 cm^{-1} , which were already mentioned above, were attributed to the stretching vibration of active phenolic hydroxy in the resin structure.

3.3. Kinetic Study of BOE/DGEBA-BOG Curing System

The curing reaction of the BOG resins with 40 wt.% BOE/DGEBA (based on the weight of the BOG resin) was performed. Figure 5 displays the DSC curves of the BOG + DGEBA/BOE curing system with a heating rate of 10 K/min. It shows a single exothermic peak for all the reactions, which corresponds to the completion of the thermal curing reaction [50]. When BOG was cured with only DGEBA, it exhibited a sharp exothermic peak. With the increase of the BOE ratio, the peak becomes smaller and flat. In addition, more information on the curing characteristics of the reaction was obtained by analyzing the DSC data and was listed in Table 3. According to the DSC curves, the curing temperature and reaction enthalpy of the BOG/DGEBA/BOE system decreased with an increasing BOE ratio. The result indicates that the curing reaction of BOG with BOE is easier than with DGEBA.

In a previous work, the novolac-epoxy resin curing system was built using the OH-epoxy reaction [54]. Furthermore, the three main reaction steps of the chain-wise polymerization curing mechanisms of the novolac-epoxy system catalyzed by TPP are initiation, propagation, and branching [38]. The exothermic peak temperature at various heating rates of the curing reactions was between 84–176 °C (Table 4). The curing onset and peak temperatures of BOG resin cured with BOE resin changed significantly compared with curing only with DGEBA.

As Figure 6 illustrates, the slope of the line fitted on the curves gives the E_a , which can be calculated by using 2 models (Equations (3) and (4)) by plotting $\ln(\beta/T_p^2)$ versus $1/T_p$ and $\log \beta$ against $1/T_p$, respectively [39]. Additionally, the reaction order (n) was determined by plotting $\ln \beta$ versus $1/T_p$ (Equation (5)), and its values are listed in Table 4. The value of the correlation coefficient (R^2), mostly greater than 0.99, allows for verifying the accuracy of the linear fitting. The overall curing reaction for all of the resins was approximately first order ($n = 0.92\text{--}0.95$), which agreed with previous studies [22,55].

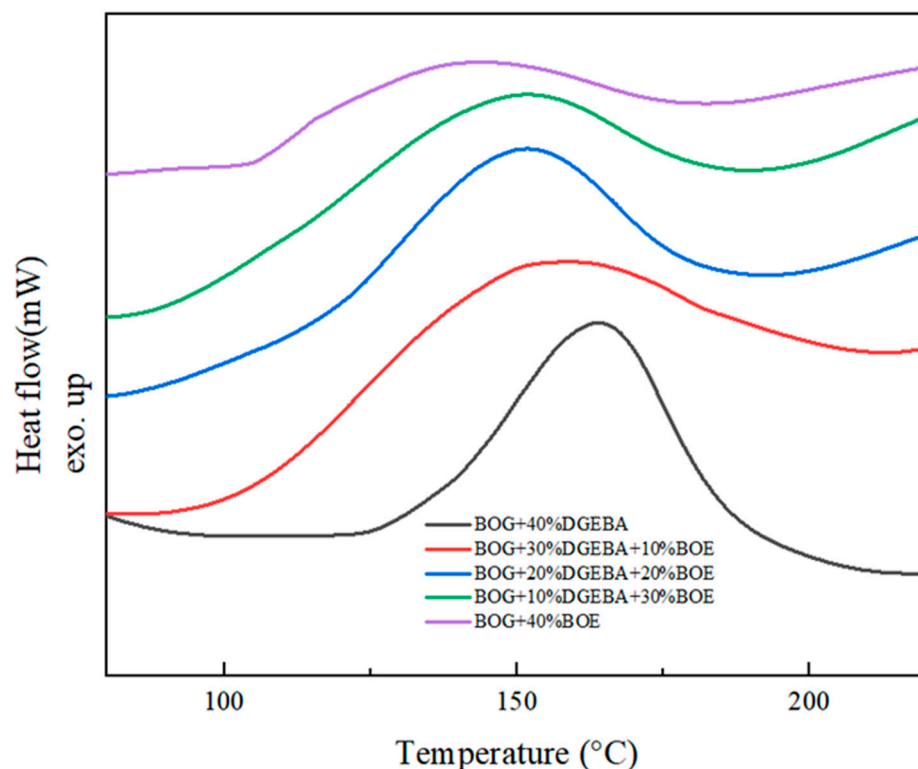


Figure 5. DSC curves of the BOG + DGEBA/BOE curing system with a heating rate of 10 K/min.

Table 3. Curing characteristics of BOG resin cured by 40 wt.% BOE resin/DGEBA at a heating rate of 10 K/min.

| Resin | Onset Temp (°C) | Peak Temp (°C) | Enthalpy (J/g) |
|---------------------------|-----------------|----------------|----------------|
| BOG + 40% DGEBA | 134.2 | 164.7 | 83.4 |
| BOG + 30% DGEBA + 10% BOE | 106.5 | 148.7 | 78.9 |
| BOG + 20% DGEBA + 20% BOE | 107.8 | 147.3 | 73.6 |
| BOG + 10% DGEBA + 30% BOE | 104.2 | 141.5 | 69.9 |
| BOG + 40% BOE | 106.1 | 135.3 | 63.1 |

Table 4. Calculated thermal curing kinetic parameters of 40 wt.% BOE resin/DGEBA cured BOG resin.

| Resin Type | | Heating Rate (K/min) | | | | E _a (kJ/mol) | | n |
|---------------------------|-----------------|----------------------|-------|-------|-------|-------------------------|------------------|------|
| | | 5 | 10 | 15 | 20 | Kissinger | Flynn–Wall–Ozawa | |
| BOG + 40% DGEBA | Onset temp (°C) | 122.2 | 134.2 | 136.9 | 139.9 | 89.5 | 92.1 | 0.95 |
| | Peak temp (°C) | 153.2 | 164.7 | 171.6 | 175.8 | | | |
| BOG + 30% DGEBA + 10% BOE | Onset temp (°C) | 104.0 | 106.5 | 116.5 | 123.9 | 76.9 | 79.8 | 0.94 |
| | Peak temp (°C) | 137.6 | 148.7 | 157.4 | 161.7 | | | |
| BOG + 20% DGEBA + 20% BOE | Onset temp (°C) | 95.7 | 107.8 | 114.9 | 119.3 | 74.2 | 77.3 | 0.93 |
| | Peak temp (°C) | 135.7 | 147.3 | 155.3 | 160.7 | | | |
| BOG + 10% DGEBA + 30% BOE | Onset temp (°C) | 84.9 | 104.2 | 114.6 | 116.1 | 73.8 | 76.7 | 0.94 |
| | Peak temp (°C) | 129.1 | 141.5 | 149.3 | 153.1 | | | |
| BOG + 40% BOE | Onset temp (°C) | 85.4 | 106.1 | 112.0 | 113.8 | 64.0 | 67.3 | 0.92 |
| | Peak temp (°C) | 121.0 | 135.3 | 142.1 | 148.2 | | | |

Consistent with the result of the curing temperature, the E_a decreased with the increase in the ratio of BOE. This result indicates that the chemical reactivity of BOE with BOG was higher than with DGEBA. The increase in the percentage of BOE created a mixture of DGEBA, and their apparent activation energy was between the two initial apparent activation energies. In correlation with the GPC result of BOE resin, it had a very high value of polydispersity. Although it possessed a larger average molecular weight, it still contained a large number of unreacted small compounds, which included many reactive functional groups, such as hydroxyl groups and aldehyde groups (Figure 3). These can bring more unoccupied reactive sites, promoting cross-linking with BOG resin compared with only using DGEBA.

3.4. Thermal Characterization of the BOE/DGEBA Cured BOG Resins

Figure 7 displays the DSC curves indicating the glass transition temperatures of the 40 wt.% of BOE/DGEBA cured BOG resins obtained. The curve of T_g gradually changed to a broader temperature range upon transition by the addition of BOE.

T_g values of the epoxy-cured BOG resins were higher than that of the uncured BOG resin (75.8 ± 1.1 °C), with a range of 96.1–121.1 °C (Table 5). However, higher proportions of BOE resulted in a lower T_g . When only BOE was used as a curing agent, the T_g reached a minimum value of 96.1 °C, probably because of the higher EEW of BOE (317.1) than DGEBA (181), and the unreacted small molecules from the bio-oil also lowered the T_g value. This result is in agreement with other research [48,50].

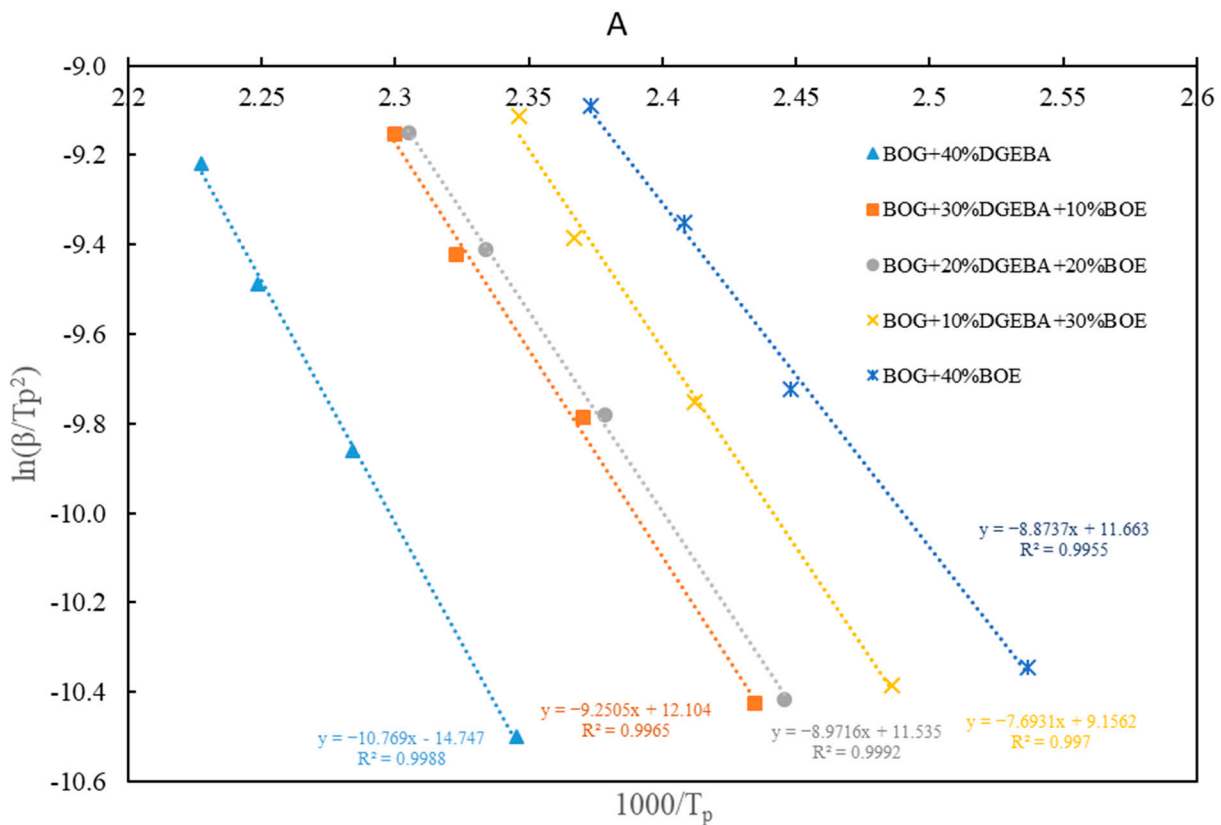


Figure 6. Cont.

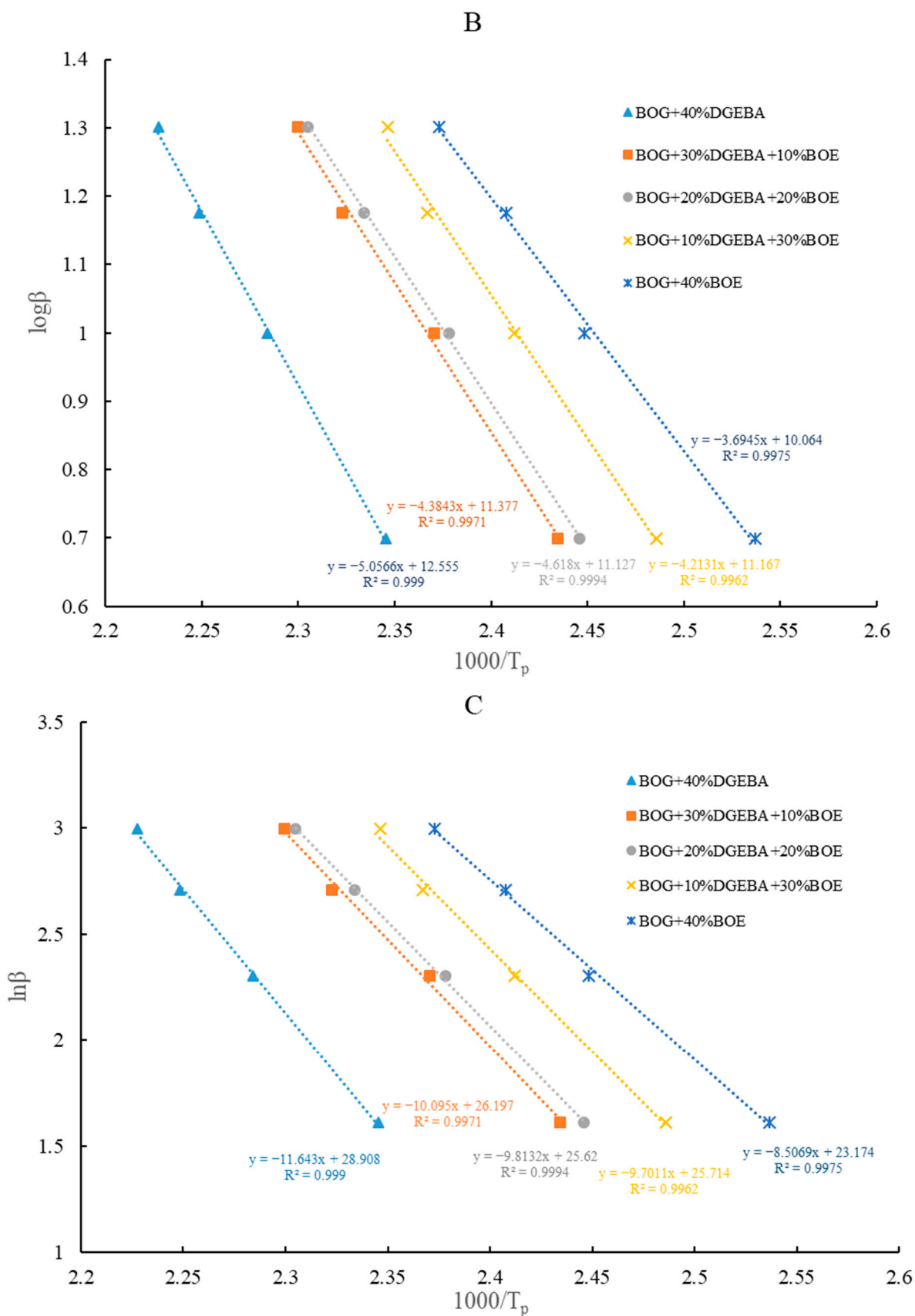


Figure 6. Plots of DSC kinetic analysis by the (A) Kissinger, (B) Ozawa equations, and (C) Crane equations.

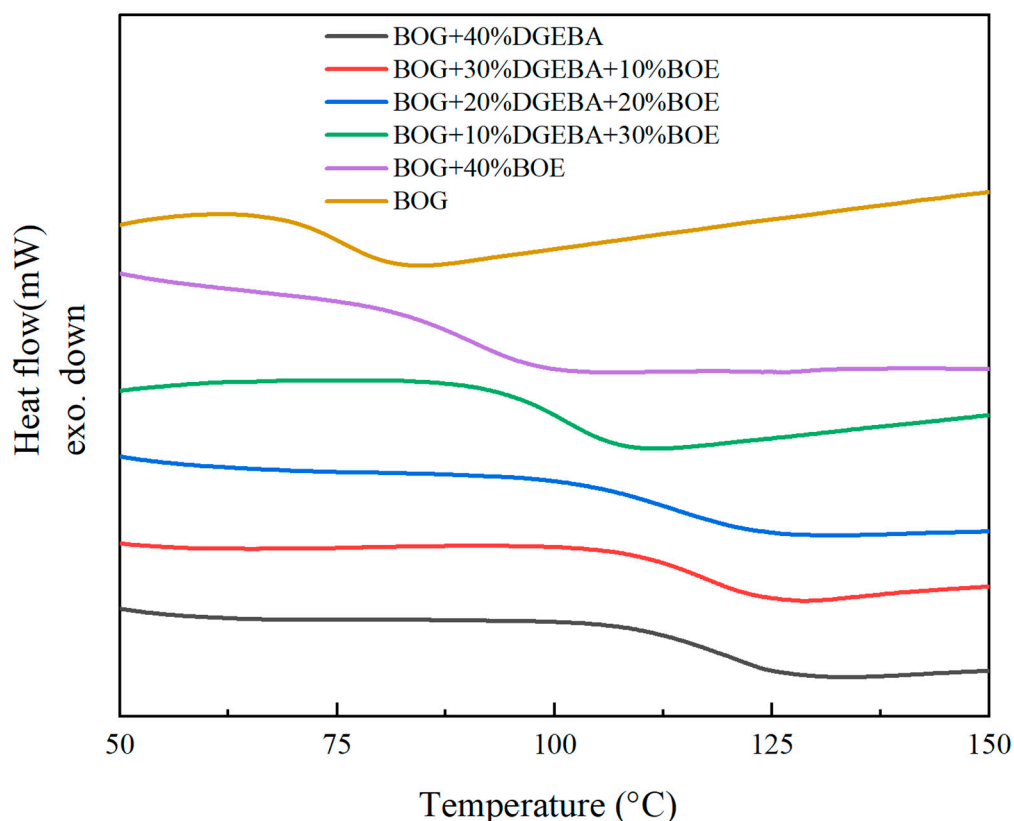


Figure 7. DSC of 40 wt.% BOE resin/DGEBA cured BOG resin.

Table 5. DSC, TGA, and DTG results of the cured BOG resin.

| Resin Name | T_g (°C) | T_{d5} (°C) | T_{max} (°C) | R_{800} (%) |
|---------------------------|-----------------|-----------------|-----------------|------------------|
| BOG | 75.8 ± 1.1 | 203.7 ± 0.8 | 335.0 ± 1.0 | 30.90 ± 0.21 |
| BOG + 40% DGEBA | 121.1 ± 0.5 | 282.9 ± 0.6 | 390.6 ± 1.7 | 39.66 ± 0.31 |
| BOG + 30% DGEBA + 10% BOE | 117.4 ± 0.8 | 282.8 ± 1.1 | 389.2 ± 2.1 | 39.99 ± 0.39 |
| BOG + 20% DGEBA + 20% BOE | 113.7 ± 0.7 | 282.4 ± 2.7 | 385.7 ± 3.3 | 40.16 ± 0.23 |
| BOG + 10% DGEBA + 30% BOE | 101.2 ± 1.5 | 278.1 ± 2.3 | 383.1 ± 1.5 | 42.29 ± 0.43 |
| BOG + 40% BOE | 96.1 ± 2.4 | 271.7 ± 1.3 | 381.5 ± 2.2 | 43.26 ± 0.57 |

Moreover, unlike DGEBA, which is a rigid molecule with only aromatic rings, BOE has both rigid and flexible connections thanks to the presence of oligomers. This flexible structure and methoxy in bio-oil may decrease the T_g of cured resins [47]. Similarly, the presence of non-phenolic compounds in the BOE may also influence the polymer T_g [34].

TGA profiles under N_2 are shown in Figure 8 in order to evaluate the thermal stability of the cured resins. Results included the initial degradation temperature for 5% weight loss (T_{d5}), the temperature of maximum decomposition rate (T_{max}), and the residue percentage at 800 °C (R_{800}), all presented in Table 5. Compared to uncured BOG resins, the thermal stability of cured resins was significantly improved, as observed by the higher values of T_{d5} , T_{max} , and R_{800} . T_{d5} and T_{max} of the cured resins decreased slightly with the decrease in DGEBA until they reached their lowest values (271.7 and 381.5, respectively) when 40% of BOE was used for curing. When a larger amount of BOE is used, a DTG peak around 271 °C is present. The decrease in the thermal stability may be attributed to the presence of methoxy groups on the aromatic ring resulting from bio-oil-derived guaiacols. The latter donates electrons to the aromatic ring, reducing thermal stability [47]. However, it can be seen in Figure 8 that the increase in the BOE proportion led to a slower thermal decomposition rate.

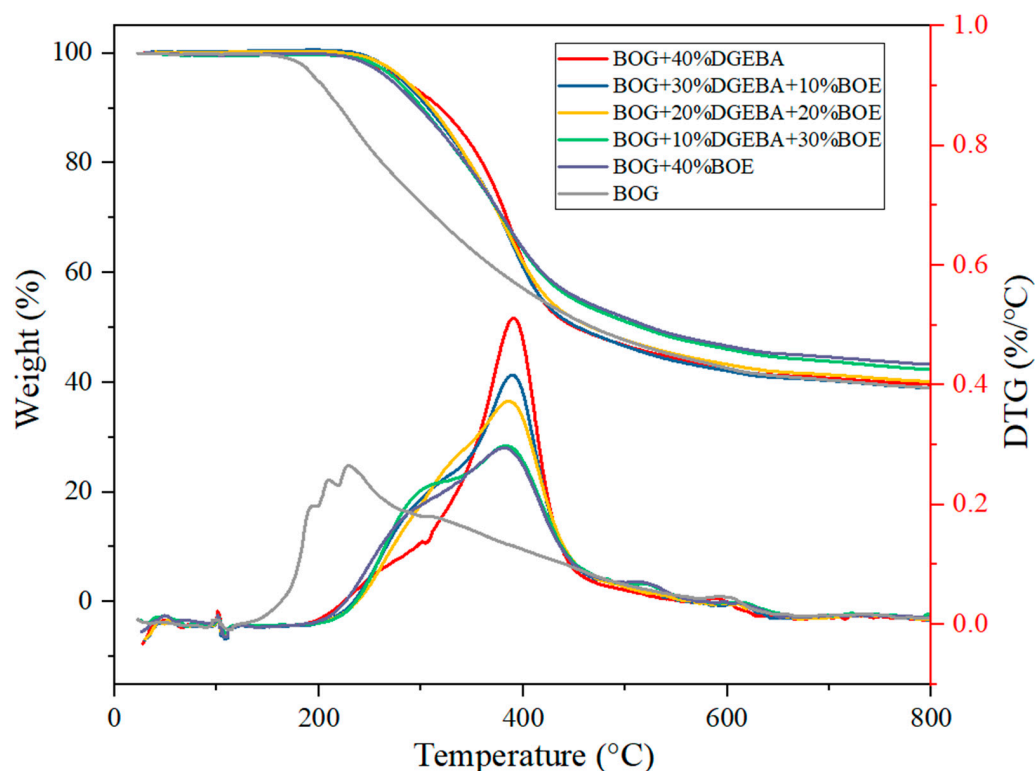


Figure 8. Thermal decomposition of 40 wt.% BOE resin/DGEBA-cured BOG resin.

The residual materials of the cured resins at 800 °C are also listed in Table 5. The presence of the BOE resin led to a significant increase in the R_{800} value of the cured resins (43.26%), which was higher than that obtained when pure DGEBA was used (39.66%); this indicates the positive effect of BOE on reducing resin decomposition, and it is attributed to the rich aromaticity in the main chain between rigid rod-like aromatics linked by carbon-carbon double bonds inherent into BOE resin from bio-oil. These polymer fragments would be transformed into char at high temperatures [50]. It also explains why BOE and BOG have more cross-linking reactions under high-temperature conditions than DGEBA.

4. Conclusions

A synthesized bio-based epoxy resin based on the upgraded beechwood pyrolysis oil was used for the first time to gradually replace the DGEBA equivalent (0–100%) as a formaldehyde-free cross-linker for bio-based novolac resin to produce a bio-based green material through this study. Incorporating the bio-based epoxy led to a lower curing reaction temperature and activation energy compared to when using a commercial curing agent (DGEBA). When the bio-based epoxy resin content increased, there were no visible effects on the degradation of cured resin. The good thermal stability of the cured resin illustrated that the synthesized epoxy resin from a biomass source is a promising green substitute for commercial DGEBA. Additional mechanical analyses would be interesting to carry out to link the thermal stability of the green material synthesized with its chemical structure.

Author Contributions: Conceptualization, J.X.; methodology, J.X., N.B. and B.T.; validation, J.X., L.A., C.M. and B.T.; formal analysis, J.X.; investigation, J.X.; resources, J.X.; data curation, J.X.; writing—original draft preparation, J.X.; writing—review and editing, J.X., N.B., C.M. and B.T.; visualization, J.X., N.B., L.A. and B.T.; supervision, B.T. and N.B. All authors have read and agreed to the published version of the manuscript.

Funding: This research received no external funding.

Data Availability Statement: The data presented in this study are available on request from the corresponding author. The data are not publicly available.

Conflicts of Interest: The authors declare no conflict of interest.

Abbreviations

| | |
|---------------------|---|
| A | Pre-exponential factor (min^{-1}) |
| BOE | Bio-oil based epoxy resin |
| BOG | Bio-oil based glyoxal novolac resin |
| BPA | Bisphenol A |
| C | Constant of Flynn–Wall–Ozawa method |
| C_{NaOH} | Molar concentration of 0.2 mol/L NaOH solution |
| DCM | Dichloromethane |
| DGEBA | Bisphenol A type epoxy resin |
| DMSO-D ⁶ | Dimethyl sulfoxide-D ⁶ |
| DSC | Differential scanning calorimeter |
| DTR | Drop tube reactor |
| ECH | Epichlorohydrin |
| EEW | Epoxy equivalent weight |
| FTIR | Fourier transform infrared spectroscopy |
| FWO | Flynn–Wall–Ozawa method |
| GC-FID | Gas chromatography with flame ionization detector |
| GC-MS | Gas chromatograph-mass spectrometry instrument |
| GPC | Gel permeation chromatography |
| ¹ H-NMR | Proton nuclear magnetic resonance |
| HMTA | Hexamethylenetetramine |
| HPLC | High-performance liquid chromatography |
| KOH | Potassium hydroxide |
| L | Weight of the dried OIL1WI |
| M | Molar concentration |
| M_n | Average molecular weight number |
| M_w | Average molecular weight |
| n | Reaction order |
| NaOH | Sodium hydroxide |
| OHN | Hydroxyl number |
| OIL1WI | Water-insoluble fractions of bio-oil products |
| OILS | Pyrolysis oil products from single condenser |
| OIL1 | Pyrolysis oil products from first condenser |
| OIL2 | Pyrolysis oil products from second condenser |
| OIL3 | Pyrolysis oil products from third condenser |
| P | BOE resin weight (g) |
| PA | Phenol acetaldehyde resin |
| PF | Phenol formaldehyde resin |
| R | Gas constant (8.314 J/mol. K) |
| R^2 | Pearson's correlation coefficient ($0 \leq R^2 \leq 1$) |
| R_{800} | Residual percentage at 800 °C |
| S | Weight of dried BOE |
| TEBAC | Benzyltriethylammonium chloride |
| T_{d5} | Initial degradation temperature for 5% weight loss |
| T_g | Glass transition temperature |
| T_{max} | Temperature of maximum decomposition rate |
| T_p | Temperature of maximum reaction rate, or peak temperature |
| TGA | Thermogravimetric analysis |
| TPP | Triphenylphosphine |
| V_A | 0.2 mol/L NaOH volume (mL) for the blank |
| V_B | 0.2 mol/L NaOH volume (mL) for the prepolymer |
| wt.% | Percentage, on mass basis |
| β | Heating rate (K/min) |

Appendix A

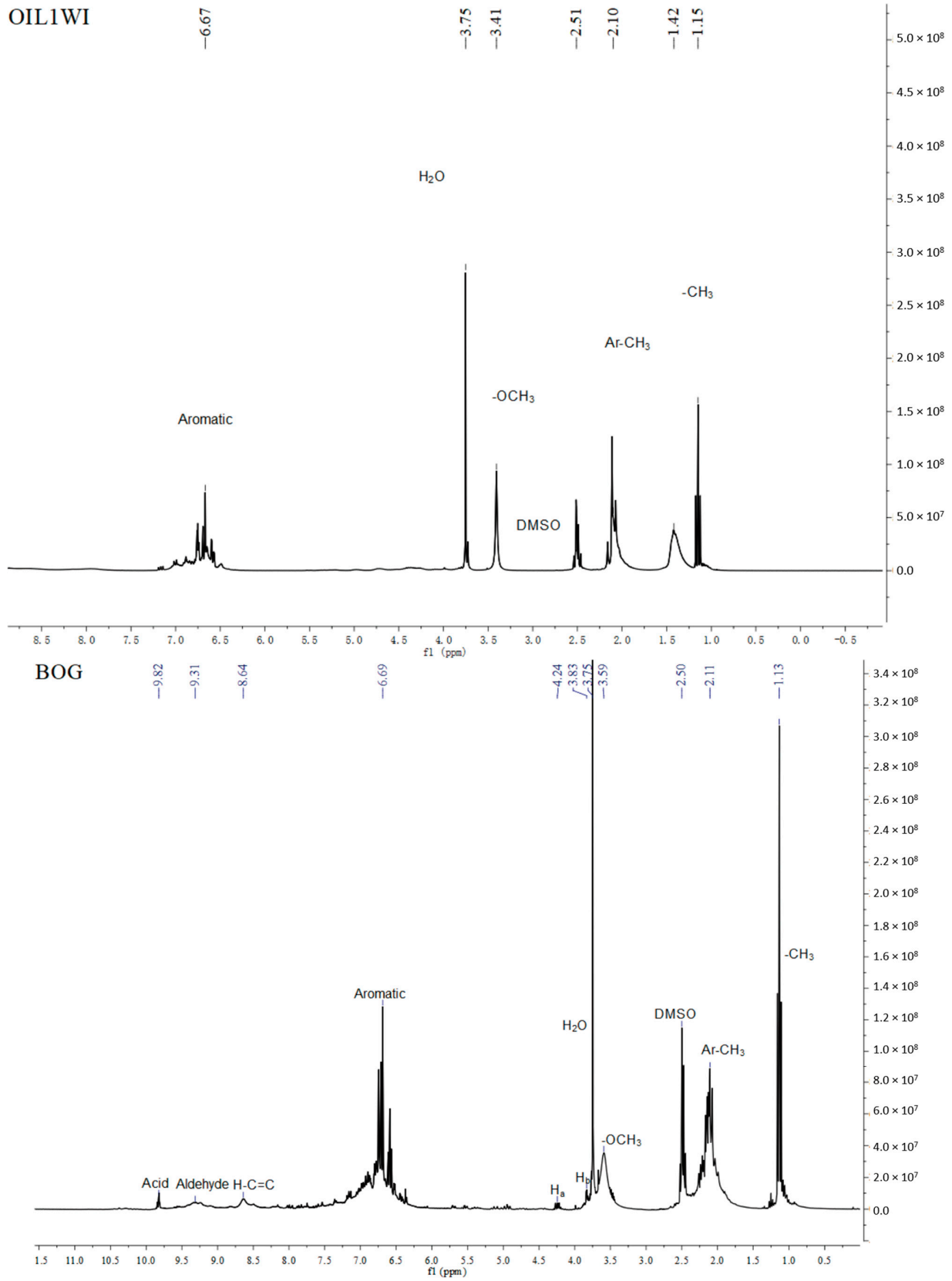


Figure A1. ¹H NMR spectra of OIL1WI and BOG resin.

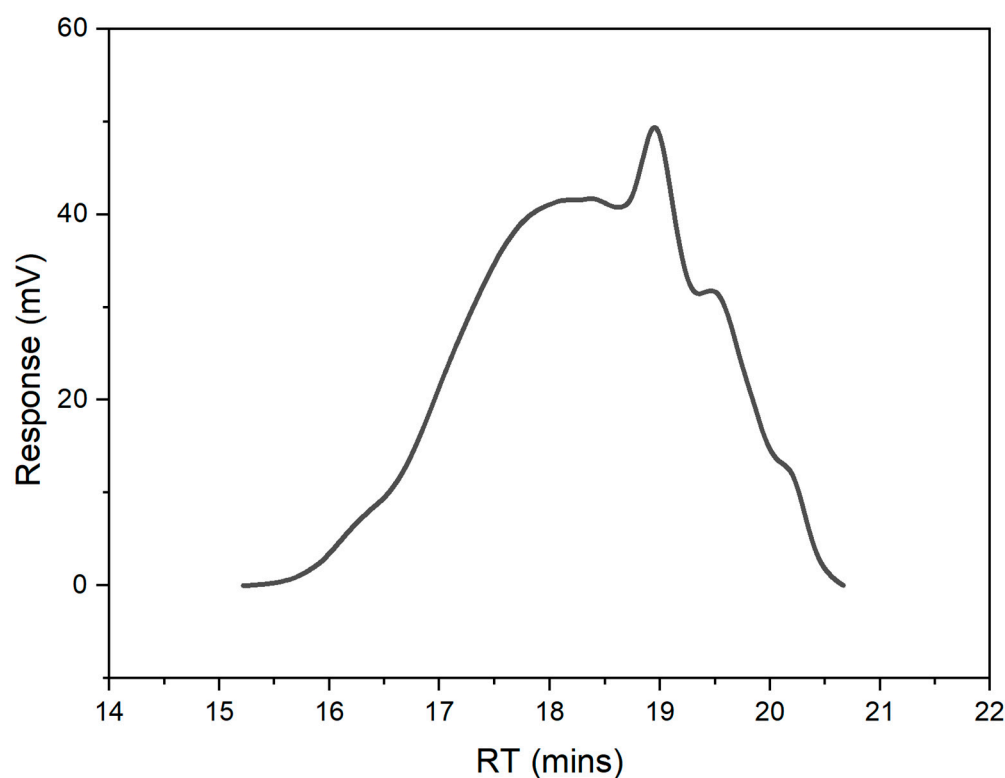


Figure A2. GPC chromatograms of BOE resin.

References

1. Ferdosian, F.; Yuan, Z.; Anderson, M.; Xu, C.C. Thermal performance and thermal decomposition kinetics of lignin-based epoxy resins. *J. Anal. Appl. Pyrolysis* **2016**, *119*, 124–132. [[CrossRef](#)]
2. Kumar, S.; Krishnan, S.; Mohanty, S.; Nayak, S.K. Synthesis and characterization of petroleum and biobased epoxy resins: A review. *Polym. Int.* **2018**, *67*, 815–839. [[CrossRef](#)]
3. Kumar, S.; Samal, S.K.; Mohanty, S.; Nayak, S.K. Recent development of biobased epoxy resins: A review. *Polym.-Plast. Technol. Eng.* **2018**, *57*, 133–155. [[CrossRef](#)]
4. Wan, J.; Zhao, J.; Zhang, X.; Fan, H.; Zhang, J.; Hu, D.; Jin, P.; Wang, D.-Y. Epoxy thermosets and materials derived from bio-based monomeric phenols: Transformations and performances. *Prog. Polym. Sci.* **2020**, *108*, 101287. [[CrossRef](#)]
5. Ding, C.; Matharu, A.S. Recent Developments on Biobased Curing Agents: A Review of Their Preparation and Use. *ACS Sustain. Chem. Eng.* **2014**, *2*, 2217–2236. [[CrossRef](#)]
6. Feghali, E.; van de Pas, D.J.; Parrott, A.J.; Torr, K.M. Biobased Epoxy Thermoset Polymers from Depolymerized Native Hardwood Lignin. *ACS Macro Lett.* **2020**, *9*, 1155–1160. [[CrossRef](#)]
7. Celikbag, Y.; Meadows, S.; Barde, M.; Adhikari, S.; Buschle-Diller, G.; Auad, M.L.; Via, B.K. Synthesis and Characterization of Bio-oil-Based Self-Curing Epoxy Resin. *Ind. Eng. Chem. Res.* **2017**, *56*, 9389–9400. [[CrossRef](#)]
8. Fang, Z.; Weisenberger, M.C.; Meier, M.S. Utilization of Lignin-Derived Small Molecules: Epoxy Polymers from Lignin Oxidation Products. *ACS Appl. Bio. Mater.* **2020**, *3*, 881–890. [[CrossRef](#)]
9. Feghali, E.; van de Pas, D.J.; Torr, K.M. Toward Bio-Based Epoxy Thermoset Polymers from Depolymerized Native Lignins Produced at the Pilot Scale. *Biomacromolecules* **2020**, *21*, 1548–1559. [[CrossRef](#)]
10. Ferdosian, F.; Yuan, Z.; Anderson, M.; Xu, C. Synthesis of lignin-based epoxy resins: Optimization of reaction parameters using response surface methodology. *RSC Adv.* **2014**, *4*, 31745–31753. [[CrossRef](#)]
11. Hernandez, E.D.; Bassett, A.W.; Sadler, J.M.; La Scala, J.J.; Stanzone, J.F. Synthesis and Characterization of Bio-based Epoxy Resins Derived from Vanillyl Alcohol. *ACS Sustain. Chem. Eng.* **2016**, *4*, 4328–4339. [[CrossRef](#)]
12. Chen, C.-H.; Tung, S.-H.; Jeng, R.-J.; Abu-Omar, M.M.; Lin, C.-H. A facile strategy to achieve fully bio-based epoxy thermosets from eugenol. *Green Chem.* **2019**, *21*, 4475–4488. [[CrossRef](#)]
13. Khundamri, N.; Aouf, C.; Fulcrand, H.; Dubreucq, E.; Tanrattanakul, V. Bio-based flexible epoxy foam synthesized from epoxidized soybean oil and epoxidized mangosteen tannin. *Ind. Crops Prod.* **2019**, *128*, 556–565. [[CrossRef](#)]
14. Benyahya, S.; Aouf, C.; Caillol, S.; Boutevin, B.; Pascault, J.P.; Fulcrand, H. Functionalized green tea tannins as phenolic prepolymers for bio-based epoxy resins. *Ind. Crops Prod.* **2014**, *53*, 296–307. [[CrossRef](#)]
15. Kim, J.R.; Sharma, S. The development and comparison of bio-thermoset plastics from epoxidized plant oils. *Ind. Crops Prod.* **2012**, *36*, 485–499. [[CrossRef](#)]

16. Pan, X.; Sengupta, P.; Webster, D.C. Novel biobased epoxy compounds: Epoxidized sucrose esters of fatty acids. *Green Chem.* **2011**, *13*, 965–975. [[CrossRef](#)]
17. Koike, T. Progress in development of epoxy resin systems based on wood biomass in Japan. *Polym. Eng. Sci.* **2012**, *52*, 701–717. [[CrossRef](#)]
18. Zhang, Y.; Pang, H.; Wei, D.; Li, J.; Li, S.; Lin, X.; Wang, F.; Liao, B. Preparation and characterization of chemical grouting derived from lignin epoxy resin. *Eur. Polym. J.* **2019**, *118*, 290–305. [[CrossRef](#)]
19. Cheng, S.; Yuan, Z.; Anderson, M.; Leitch, M.; Xu, C.C. Synthesis of biobased phenolic resins/adhesives with methylolated wood-derived bio-oil. *J. Appl. Polym. Sci.* **2012**, *126*, E431–E441. [[CrossRef](#)]
20. Mohabeer, C.; Abdelouahed, L.; Marcotte, S.; Taouk, B. Comparative analysis of pyrolytic liquid products of beech wood, flax shives and woody biomass components. *J. Anal. Appl. Pyrolysis* **2017**, *127*, 269–277. [[CrossRef](#)]
21. Aslan, M.; Özbay, G.; Ayrilmis, N. Adhesive characteristics and bonding performance of phenol formaldehyde modified with phenol-rich fraction of crude bio-oil. *J. Adhes. Sci. Technol.* **2015**, *29*, 2679–2691. [[CrossRef](#)]
22. Cheng, S.; D’Cruz, I.; Yuan, Z.; Wang, M.; Anderson, M.; Leitch, M.; Xu, C.C. Use of biocrude derived from woody biomass to substitute phenol at a high-substitution level for the production of biobased phenolic resol resins. *J. Appl. Polym. Sci.* **2011**, *121*, 2743–2751. [[CrossRef](#)]
23. Cui, Y.; Chang, J.; Wang, W. Fabrication of Glass Fiber Reinforced Composites Based on Bio-Oil Phenol Formaldehyde Resin. *Materials* **2016**, *9*, 886. [[CrossRef](#)] [[PubMed](#)]
24. Cui, Y.; Hou, X.; Wang, W.; Chang, J. Synthesis and Characterization of Bio-Oil Phenol Formaldehyde Resin Used to Fabricate Phenolic Based Materials. *Materials* **2017**, *10*, 668. [[CrossRef](#)]
25. Wang, J.; Abdelouahed, L.; Xu, J.; Brodu, N.; Taouk, B. Catalytic Hydrodeoxygenation of Model Bio-oils Using HZSM-5 and Ni2P/HZM-5 Catalysts: Comprehension of Interaction. *Chem. Eng. Technol.* **2021**, *44*, 2126–2138. [[CrossRef](#)]
26. Xu, J.; Brodu, N.; Wang, J.; Abdelouahed, L.; Taouk, B. Chemical characteristics of bio-oil from beech wood pyrolysis separated by fractional condensation and water extraction. *J. Energy Inst.* **2021**, *99*, 186–197. [[CrossRef](#)]
27. Oasmaa, A.; Kuoppala, E.; Gust, S.; Solantausta, Y. Fast Pyrolysis of Forestry Residue. 1. Effect of Extractives on Phase Separation of Pyrolysis Liquids. *Energy Fuels* **2003**, *17*, 1–12. [[CrossRef](#)]
28. Zhang, X.; Ma, H.; Wu, S.; Jiang, W.; Wei, W.; Lei, M. Fractionation of pyrolysis oil derived from lignin through a simple water extraction method. *Fuel* **2019**, *242*, 587–595. [[CrossRef](#)]
29. Liu, Y.; Via, B.K.; Pan, Y.; Cheng, Q.; Guo, H.; Auad, M.L.; Taylor, S. Preparation and Characterization of Epoxy Resin Cross-Linked with High Wood Pyrolysis Bio-Oil Substitution by Acetone Pretreatment. *Polymers* **2017**, *9*, 106. [[CrossRef](#)]
30. Zhang, P.; Wang, S.; Zhang, X.; Jing, X. The effect of free dihydroxydiphenylmethanes on the thermal stability of novolac resin. *Polym. Degrad. Stab.* **2019**, *168*, 108946. [[CrossRef](#)]
31. Zhang, Y.; Yuan, Z.; Xu, C. Bio-based resins for fiber-reinforced polymer composites. In *Natural Fiber-Reinforced Biodegradable and Bioresorbable Polymer Composites*; Woodhead Publishing: Sawston, UK, 2017; pp. 137–162.
32. Xu, J.; Brodu, N.; Mignot, M.; Youssef, B.; Taouk, B. Synthesis and characterization of phenolic resins based on pyrolysis bio-oil separated by fractional condensation and water extraction. *Biomass Bioenergy* **2022**, *159*, 106393. [[CrossRef](#)]
33. Xu, J.; Brodu, N.; Abdelouahed, L.; Taouk, B. Investigation of the combination of fractional condensation and water extraction for improving the storage stability of pyrolysis bio-oil. *Fuel* **2022**, *314*, 123019. [[CrossRef](#)]
34. Aouf, C.; Benyahya, S.; Esnouf, A.; Caillol, S.; Boutevin, B.; Fulcrand, H. Tara tannins as phenolic precursors of thermosetting epoxy resins. *Eur. Polym. J.* **2014**, *55*, 186–198. [[CrossRef](#)]
35. Barde, M.; Adhikari, S.; Via, B.K.; Auad, M.L. Synthesis and characterization of epoxy resins from fast pyrolysis bio-oil. *Green Mater.* **2018**, *6*, 76–84. [[CrossRef](#)]
36. Wang, F.; Kuai, J.; Pan, H.; Wang, N.; Zhu, X. Study on the demethylation of enzymatic hydrolysis lignin and the properties of lignin–epoxy resin blends. *Wood Sci. Technol.* **2018**, *52*, 1343–1357. [[CrossRef](#)]
37. Choi, W.S.; Shanmugaraj, A.M.; Ryu, S.H. Study on the effect of phenol anchored multiwall carbon nanotube on the curing kinetics of epoxy/Novolac resins. *Thermochim. Acta* **2010**, *506*, 77–81. [[CrossRef](#)]
38. Ren, S.-P.; Lan, Y.-X.; Zhen, Y.-Q.; Ling, Y.-D.; Lu, M.-G. Curing reaction characteristics and phase behaviors of biphenol type epoxy resins with phenol novolac resins. *Thermochim. Acta* **2006**, *440*, 60–67. [[CrossRef](#)]
39. Zhang, Y.; Ferdosian, F.; Yuan, Z.; Xu, C.C. Sustainable glucose-based phenolic resin and its curing with a DGEBA epoxy resin. *J. Taiwan Inst. Chem. Eng.* **2017**, *71*, 381–387. [[CrossRef](#)]
40. Böhm, R.; Hauptmann, M.; Pizzi, A.; Friedrich, C.; Laborie, M.-P. The chemical, kinetic and mechanical characterization of tannin-based adhesives with different crosslinking systems. *Int. J. Adhes. Adhes.* **2016**, *68*, 1–8. [[CrossRef](#)]
41. Hussin, M.H.; Samad, N.A.; Latif, N.H.A.; Rozuli, N.A.; Yusoff, S.B.; Gambier, F.; Brosse, N. Production of oil palm (*Elaeis guineensis*) fronds lignin-derived non-toxic aldehyde for eco-friendly wood adhesive. *Int. J. Biol. Macromol.* **2018**, *113*, 1266–1272. [[CrossRef](#)]
42. Aziz, N.A.; Latip, A.F.A.; Peng, L.C.; Latif, N.H.A.; Brosse, N.; Hashim, R.; Hussin, M.H. Reinforced lignin-phenol-glyoxal (LPG) wood adhesives from coconut husk. *Int. J. Biol. Macromol.* **2019**, *141*, 185–196. [[CrossRef](#)] [[PubMed](#)]
43. Aouf, C.; Le Guernevé, C.; Caillol, S.; Fulcrand, H. Study of the O-glycidylation of natural phenolic compounds. The relationship between the phenolic structure and the reaction mechanism. *Tetrahedron* **2013**, *69*, 1345–1353. [[CrossRef](#)]

44. Sibaja, B.; Adhikari, S.; Celikbag, Y.; Via, B.; Auad, M.L. Fast pyrolysis bio-oil as precursor of thermosetting epoxy resins. *Polym. Eng. Sci.* **2018**, *58*, 1296–1307. [[CrossRef](#)]
45. Hussin, M.H.; Aziz, A.A.; Iqbal, A.; Ibrahim, M.N.M.; Latif, N.H.A. Development and characterization novel bio-adhesive for wood using kenaf core (*Hibiscus cannabinus*) lignin and glyoxal. *Int. J. Biol. Macromol.* **2019**, *122*, 713–722. [[CrossRef](#)] [[PubMed](#)]
46. Nahra, L.R.; Rezende, M.C.; Oliveira, M.P.; Guerrini, L.M. Glyoxalation of Kraft lignin and optimization of electrospinning process parameters for producing polyacrylonitrile/KL nanomats for potential applications as carbon material. *J. Polym. Res.* **2020**, *27*, 331. [[CrossRef](#)]
47. van de Pas, D.J.; Torr, K.M. Biobased Epoxy Resins from Deconstructed Native Softwood Lignin. *Biomacromolecules* **2017**, *18*, 2640–2648. [[CrossRef](#)]
48. Ma, S.; Liu, X.; Fan, L.; Jiang, Y.; Cao, L.; Tang, Z.; Zhu, J. Synthesis and properties of a bio-based epoxy resin with high epoxy value and low viscosity. *ChemSusChem* **2014**, *7*, 555–562. [[CrossRef](#)]
49. Nouailhas, H.; Aouf, C.; Le Guerneve, C.; Caillol, S.; Boutevin, B.; Fulcrand, H. Synthesis and properties of biobased epoxy resins. part 1. Glycidylation of flavonoids by epichlorohydrin. *J. Polym. Sci. Part A Polym. Chem.* **2011**, *49*, 2261–2270. [[CrossRef](#)]
50. Shang, L.; Zhang, X.; Zhang, M.; Jin, L.; Liu, L.; Xiao, L.; Li, M.; Ao, Y. A highly active bio-based epoxy resin with multi-functional group: Synthesis, characterization, curing and properties. *J. Mater. Sci.* **2017**, *53*, 5402–5417. [[CrossRef](#)]
51. Wang, Z.; Gnanasekar, P.; Nair, S.S.; Farnood, R.; Yi, S.; Yan, N. Biobased Epoxy Synthesized from a Vanillin Derivative and Its Reinforcement Using Lignin-Containing Cellulose Nanofibrils. *ACS Sustain. Chem. Eng.* **2020**, *8*, 11215–11223. [[CrossRef](#)]
52. Kuo, P.-Y.; de Assis Barros, L.; Sain, M.; Tjong, J.S.Y.; Yan, N. Effects of Reaction Parameters on the Glycidyl Etherification of Bark Extractives during Bioepoxy Resin Synthesis. *ACS Sustain. Chem. Eng.* **2016**, *4*, 1016–1024. [[CrossRef](#)]
53. Ramires, E.C.; Megiatto, J.D., Jr.; Gardrat, C.; Castellan, A.; Frollini, E. Biobased composites from glyoxal-phenolic resins and sisal fibers. *Bioresour. Technol.* **2010**, *101*, 1998–2006. [[CrossRef](#)]
54. Nair, C. Advances in addition-cure phenolic resins. *Prog. Polym. Sci.* **2004**, *29*, 401–498. [[CrossRef](#)]
55. Wang, M.; Wei, L.; Zhao, T. Cure study of addition-cure-type and condensation–addition-type phenolic resins. *Eur. Polym. J.* **2005**, *41*, 903–912. [[CrossRef](#)]

Disclaimer/Publisher’s Note: The statements, opinions and data contained in all publications are solely those of the individual author(s) and contributor(s) and not of MDPI and/or the editor(s). MDPI and/or the editor(s) disclaim responsibility for any injury to people or property resulting from any ideas, methods, instructions or products referred to in the content.